Defence Research and Development Canada
Recherche et développement pour la défense Canada

DEFENCE R&D DÉFENSE

Current flow through two dimensional arrays of metal nanoparticles as a novel sensor platform

D.B. Pedersen and S. Wang

Defence R&D Canada

Technical Memorandum

DRDC Suffield TM 2009-068

May 2009

Canada

Current flow through two dimensional arrays of metal nanoparticles as a novel sensor platform

D. B. Pedersen, S. Wang
Defence R&D Canada – Suffield

Defence R&D Canada – Suffield

Technical Memorandum

DRDC Suffield TM 2009-068

May 2009

Principal Author

Original signed by David B. Pedersen

David B. Pedersen

Approved by

Original signed by Clement Laforce

Clement Laforce
Head/HPS

Approved for release by

Original signed by Paul D'Agostino

Paul D'Agostino
Head/Document Review Panel

Abstract

Exposure of nanoparticles of Ag to 2-CEES (2-chloroethyl ethylsulfide, a simulant of the sulfur mustard warfare agent) was found to cause a significant change in the film conduction characteristics that could be used as a sensitive method of detection. Ag nanoparticles deposited onto highly-ordered pyrolitic graphite, glass, and polyethylene substrates were found to form such films. Uptake of 2-CEES was irreversible and cumulative. The sensitivity and cumulative nature make the nanoparticle films most appealing as personal exposure indicators.

Résumé

On a trouvé que l'exposition de nanoparticules de Ag au 2-CEES (le sulfure de 2-chloroéthyle et d'éthyle, un simulant de l'agent de guerre, moutarde au souffre) cause un changement important dans les caractéristiques de conduction du film et qu'elle pouvait être utilisée comme une méthode sensible de détection. On a trouvé que les nanoparticules Ag déposées sur du graphite pyrolytique de qualité élevée, du verre et des substrats de polyéthylène, formaient de tels films. L'implantation de 2-CEES était irréversible et cumulative. La nature sensible et cumulative des films de nanoparticules rend ces derniers très attrayants comme indicateurs personnels d'exposition.

This page intentionally left blank.

Executive summary

Current flow through two dimensional arrays of metal nanoparticles as a novel sensor platform

D. B. Pedersen, S. Wang; DRDC Suffield TM 2009-068; Defence R&D Canada – Suffield; May 2009.

Personal badge-type exposure indicators are critical components of next generation protective gear. Ideally, such sensors not only warn of an exposure event but also quantify it and provide a stream of data in real time so that informed decisions can be made regarding the toxicity of the soldier's environment. As a novel approach to this problem, films of metal nanoparticles deposited onto glass and polyethylene substrates have been made. When exposed to gases, the properties of such films changed. Specifically, there is a measureable change in the resistance to current flow through nanoparticle ensembles spanning the space between, and in electrical contact with, two electrodes. For a sulfur mustard simulant, 2-chloroethyl ethylsulfide (2-CEES), the resistance change was over an order of magnitude. This large change reflects a high sensitivity. Furthermore, for 2-CEES the nanoparticle films functioned as cumulative sensors; the resistance changed steadily over the duration of the exposure. The resistance measured therefore reflects the total dose, which is related to the concentration-time data used to determine toxicity. This feature, combined with portability, low power requirements, and high sensitivity, make these nanoparticle films very appealing as next generation personal badge-type exposure indicators. In this technical memorandum, the initial studies of the response of the nanoparticle films to 2-CEES are reported.

Sommaire

Current flow through two dimensional arrays of metal nanoparticles as a novel sensor platform

D. B. Pedersen, S. Wang; DRDC Suffield TM 2009-068; R & D pour la défense Canada – Suffield; mai 2009.

Les indicateurs d'exposition de type macarons sont une composante essentielle de la génération future des tenues de protection. Idéalement, de tels capteurs non seulement avertissent de l'événement d'exposition mais ils quantifient aussi cette dernière et procure une suite de données en temps réel permettant la prise de décisions éclairées au sujet de la toxicité de l'environnement du soldat. On a récemment expérimenté pour mieux résoudre ce problème en déposant des nanoparticules de métal sur du verre et des substrats de polyéthylène pour créer des films. Les propriétés de ces films ont changé dès que ces derniers ont été exposés à des gaz. On a spécifiquement remarqué un changement mesurable dans la résistance de l'intensité du courant à travers l'ensemble des nanoparticules s'étalant sur tout l'espace et en contact électrique avec deux électrodes. Pour le simulant de la moutarde au souffre, le sulfure de 2-chloroéthyle et d'éthyle (2-CEES), le changement de la résistance était d'un ordre de grandeur. Ce changement important reflète une grande sensibilité. De plus, concernant les 2-CEES, les films fonctionnaient comme des capteurs cumulatifs ; la résistance changeait de façon constante pendant la durée de l'exposition. De cette manière, la résistance mesurée reflète la dose totale qui est liée aux données de concentration et de durée utilisées pour déterminer la toxicité. Cette caractéristique combinée à la portabilité, au besoin faible en électricité et à la grande sensibilité fait que ces films de nanoparticules sont très attrayants comme génération future des indicateurs d'exposition de type macaron personnel. Les études initiales de réponse des films de nanoparticules aux 2-CEES sont documentées dans ce document technique.

Table of contents

List of figures

1 Introduction

The current flow between metal nanoparticles interconnected by molecules is a fundamental process underlying single electron transistors and much of the field of molecular electronics [1–4]. When the distance between nanoparticles is greater than 2 nm and the barrier to charge transfer greater than 1 eV, current flow between particles occurs via single-electron tunnelling [5]. Under these conditions, the residence time of the electron on a nanoparticle is relatively long and electric current flow occurs via a series of discrete tunnelling "hops" of electrons from nanoparticle to nanoparticle. In this regime, the rate of current flow depends on a number of factors including the bias applied, the electronic structure of the interparticle molecules, the quality of the electrical contact between the molecules and the surface of the nanoparticles, the distance between nanoparticles, and the charging energy of the nanoparticles (see Fig. 1) [3, 4, 6, 7].

Current flow through monolayers of close-packed metal nanoparticles have been extensively studied. Examples studied to date include films of thiol-capped 2.7–4.8 nm diameter Ag nanoparticles [8–10], and monolayer-protected gold nanoparticles [11–13]. The nanoparticles in such films are typically encapsulated in monolayer coatings, which prevent particle coalescence as well as retention of a constant and well defined interparticle spacing (see Fig. 1). The formation of films from the coated nanoparticles occurs via self-assembly [4]. The resulting bilayer of molecules between the nanoparticles in such films provides a barrier to direct charge transport between particles, ensuring that interparticle, single-electron tunnelling of charge between the nanoparticles is the dominant charge transfer mechanism (Fig. 1). In this configuration, the conduction characteristics of the nanoparticle film are expected to be especially sensitive to the nature of the material between particles [14, 15]. Self-assembly methods, however, are not ideally suited for study of conduction through molecules because changing the type of molecule also changes the interparticle spacing, so the results are convoluted. To circumvent this problem, and gain a clearer understanding of the effect of monolayers of molecules on current flow between nanoparticles, we have instead focused on films of naked nanoparticles. Using a gas-phase deposition approach [16, 17], monolayers of ligand-free nanoparticles can be generated in which the average interparticle distance is controllable. When the interparticle distance is small enough, these naked nanoparticle films also display conduction behaviours characteristic of single-electron tunnelling through the spaces between the particles [18]. Because the electrons necessarily tunnel through the interparticle space, the addition of molecular material to these spaces (most likely as an adsorbate on the nanoparticle surfaces) is found to impact the tunnelling rate and current flow observed. This approach allows the current flow through ligand-free nanoparticle assemblies to be compared with molecule-exposed analogues directly. Thus the medium through which the electron tunnels can be changed without changing the interparticle spacing. Accordingly, these systems are ideally suited for studying the effect of adsorbed molecules on tunnelling currents between nanoparticles.

In this paper we present a first look at the effect of adsorbates on tunnelling current flow through naked nanoparticle films. 2-Chloroethyl ethyl sulfide (2-CEES) is a simulant of sulfur mustard warfare agent, bis(2-chloroethyl) sulfide. 2-CEES adsorbate was added by

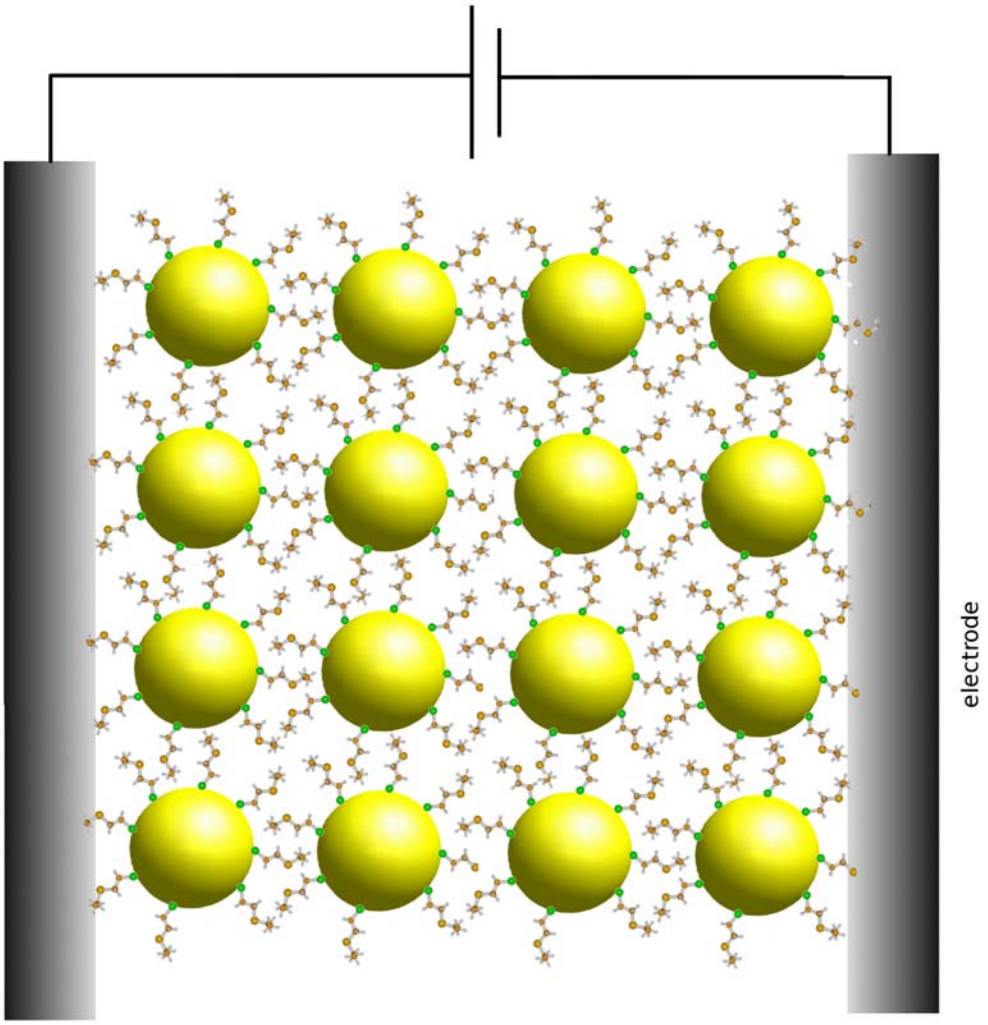

Figure 1: *Diagram of the circuit formed by an array of monolayer-coated metal nanoparticles coupled to two electrodes. A bias applied across the nanoparticles causes current to flow via single-electron tunnelling events between particles. See text for details.*

exposing nanoparticle films to 2-CEES vapour. Adsorption was found to change the nature of the inter-nanoparticle medium significantly, as reflected in measures of the tunnelling current and film conduction characteristics. We find that these changes can be monitored as a sensitive way of "sensing" the presence of the adsorbate. In this paper we demonstrate the feasibility of using measurements of current flow across monolayer films of naked nanoparticles as the basis of a novel sensor platform.

2 Experimental section

The nanoparticle deposition apparatus has been described elsewhere [19]. Nanoparticles were first generated in the gas phase using a magnetron DC-sputtering source. Application of a 280 V bias between an anode cap and a metal target caused a discharge in the 0.17 Torr pressure of Ar gas maintained between them. The current flow to the discharge was kept to 200 mA. Any Ar^+ ions generated in the discharge were accelerated toward the negatively biased metal target which they struck with force, thus liberating metal atoms to the gas phase. These atoms were swept up in the flow of Ar leaving the discharge region. Upon leaving the sputtering region the atoms passed through an aggregation zone where the collision frequency between metal atoms was high, and formation of nanoparticles occurred. The nanoparticles thus generated then moved downstream into the expansion zone, which was evacuated by a 500 L s^{-1} turbo pump (Varian V-550). The nanoparticles then passed through an orifice into the neighbouring deposition chamber where a pressure of $<10^{-4}$ Torr was maintained during deposition by a 300 L s^{-1} turbo pump (Varian TV-301). The size of the nanoparticles could be varied by varying parameters such as Ar and He gas flow rates, aggregation zone length, and discharging current. A substrate (polyethylene or glass) with painted silver electrodes (see Fig. 3), positioned in front of the orifice, collected the nanoparticles, which deposited as 2D films of naked nanoparticles. The distance between the particles varied with deposition time pseudo-continuously; at longer times more particles reside on the surface and the average interparticle distance is decreased accordingly. The resistance between electrodes was monitored during deposition with an Agilent digital multimeter (34401A) connected to a computer via HPIB interface.

A scanning tunnelling microscope (STM) was used to acquire images of the nanoparticles. Nanoparticle films for STM imaging were prepared in the same way as other samples but deposited onto highly ordered pyrolytic graphite (HOPG) instead of polyethlyene or glass. The STM routinely produces images of HOPG with single atom resolution.

Exposure experiments were conducted in a fume hood. Light exiting an optic fibre connected to a halogen lamp passed through the sample and was collected by a collimating lens attached to a second optic fibre, on the other side of the sample, that carried the light to the CCD array of a UV-vis spectrometer (Ocean Optics SD2000). In this configuration, the resistance between electrodes and the optical spectrum of the nanoparticles between electrodes could be monitored simultaneously during exposure of the nanoparticle film to 2-CEES. Exposure was effected by opening a bottle of 2-CEES (Aldrich, 98%) 5 cm from the film and letting the vapours diffuse in the fume hood.

3 Results and Discussion

The deposition of Ag nanoparticles generated by the sputtering source onto substrates yielded two dimensional arrays of nanoparticles. A sample scanning electron microscope (SEM) image is shown in Fig. 2A. As seen, the particles are monodispersed in a monolayer with no evidence of particle aggregation or coalescence. In Fig. 2B, a scanning tunnelling microscope (STM) image of a film deposited on highly ordered pyrolitic graphite (HOPG) is shown. The particles appear as bright spots against a darker background. The outline of each particle is discernible and the size easily determined. From such images the 2D nature of the films was established and the diameter of the nanoparticles was found to be 3.2 ± 0.5 nm. The distance between particles could be varied by varying the deposition time, t. In Fig. 2, for example, the distance between the nanoparticles was found to be $>$20 nm but smaller interparticle separation was possible by increasing the deposition time. In general, the interparticle separation has a well defined *average* value because the number of particles on the substrate increases linearly with time. It is straightforward to show that such a deposition process yields an *average* interparticle separation that varies inversely with $t^{\frac{1}{2}}$, where t is the deposition time. Accordingly, plots of the interparticle distance versus the inverse of the square root of the deposition time are linear [19]. The linearity combined with STM data and trends in the optical properties of such films [18, 19] establish that the films are 2D arrays of nanoparticles with interparticle distances that decrease steadily as deposition time is increased.

For a 15 min deposition of Ag nanoparticles on a glass slide or polyethylene film, the average interparticle distance is small enough that current can flow between two silver electrodes situated at either end of the nanoparticle film (see Fig. 3). When the particle density is low enough, such current is expected to flow via tunnelling of electrons across the interparticle gaps. Controlling the distance between adjacent nanoparticles affords an opportunity to examine the distance dependence of the through–space tunnelling current between nanoparticles. A plot of the resistance, measured between two silver electrodes spaced 3 mm apart on the surface of a polyethylene film, versus t is shown in Fig. 4. These data were collected in situ during deposition of the nanoparticles on the polyethylene surface. Similar results were obtained on glass. Early on in the deposition the resistance is infinite. As the particle density in the film increases it eventually reaches a critical value where a resistance and current flow is measurable. The average spacing between nanoparticles (i.e. centre to centre) at this time is greater than 50 nm, as determined by STM imaging of nanoparticles deposited on HOPG under identical conditions. At this distance, there is no direct, conducting path for electrons to follow and current flow occurs via tunnelling of electrons between adjacent nanoparticles. As the distance between particles decreases further the tunnelling rate increases and the resistance measured between electrodes decreases, as seen in Fig. 4.

The tunnelling current, or rate of tunnelling, is given by

$$I = I_0 e^{-\beta d} \tag{1}$$

where I_0 is the pre-exponential factor, d is the interparticle separation, and β is the fall–

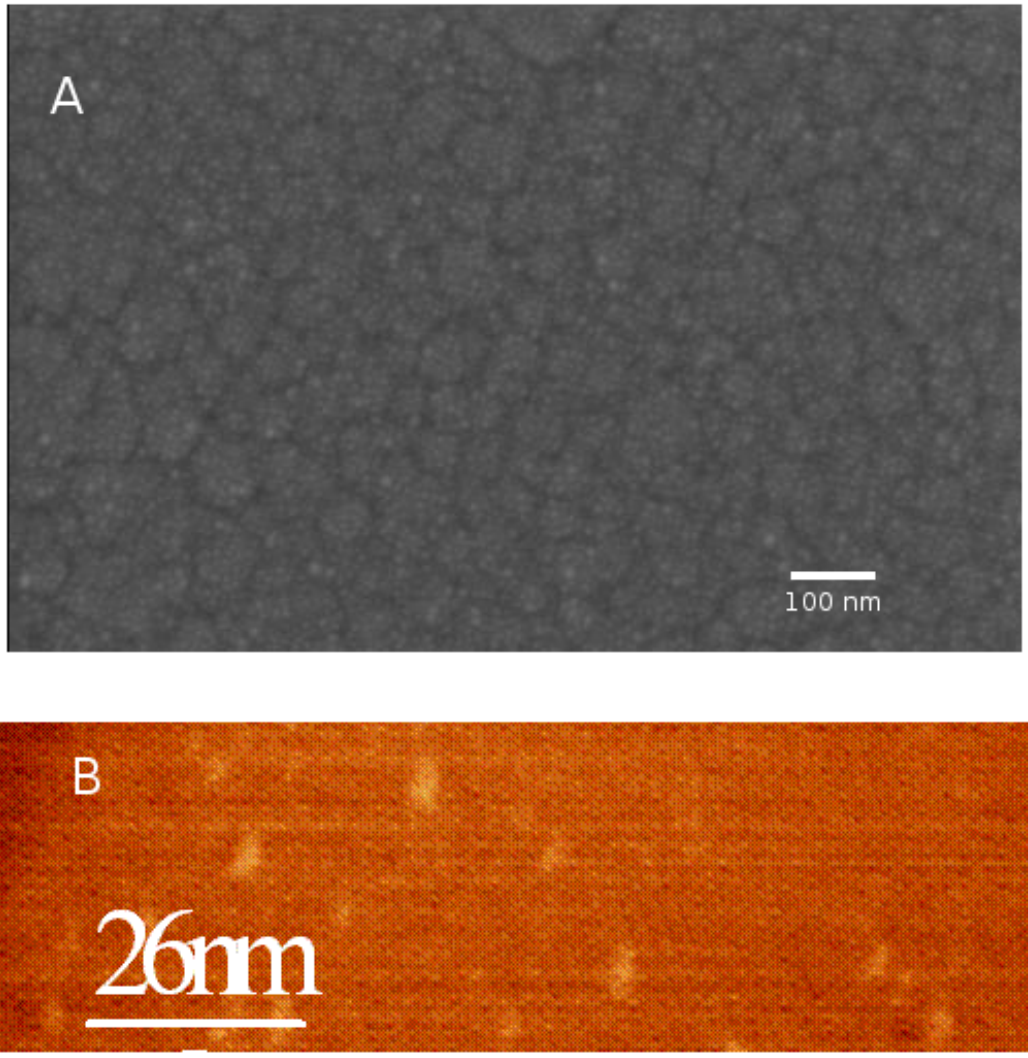

Figure 2: *A scanning electron microscope image of a nanoparticle film is shown in Panel A. In Panel B a scanning tunnelling microscope image of a lower density Ag nanoparticle film is shown. In this image, individual nanoparticles appear as light spots against the darker HOPG background. The scale bar is shown. The average particle diameter is 3.2 ± 0.5 nm. The deposition time is 150 s.*

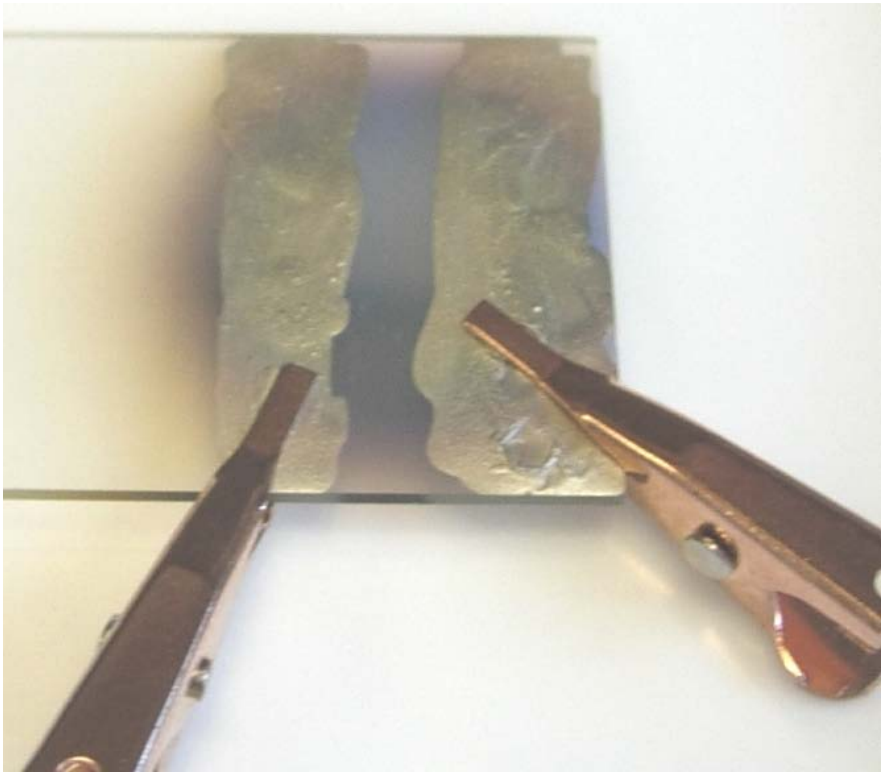

Figure 3: *A Ag nanoparticle film on glass. The alligator clips are shown connected to the Ag electrodes that were painted on prior to deposition. The nanoparticle film appears between the electrodes as a dark blue film that fades to brownish yellow at the edges. The deposition time was 15 min.*

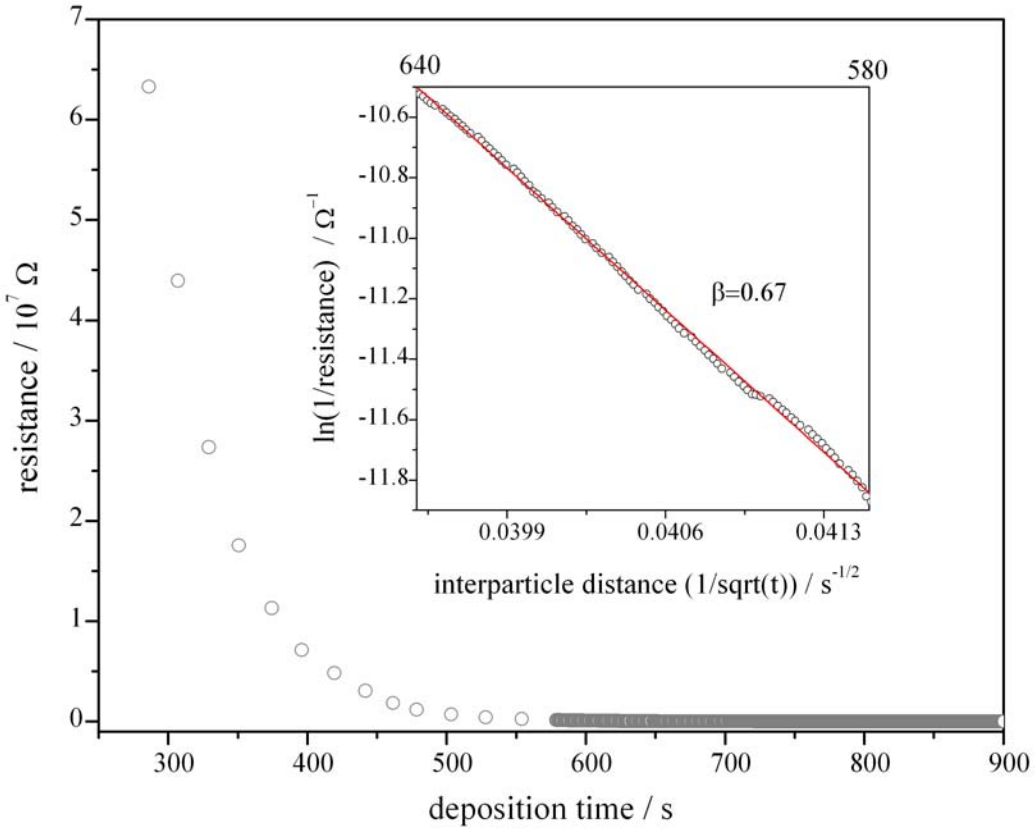

Figure 4: *Plot of the resistance, between two Ag electrodes painted onto a 5 μm thick polyethylene film, versus deposition time. The electrodes were 3 mm apart. For each point in the early part of the deposition, the sputtering source was turned off so that the current flow associated with the deposition of the 3.2 $\pm$ 0.5 nm diameter Ag nanoparticle ions onto the polyethylene film did not affect the resistance measured. After 580 s, data were obtained continuously with the source on because this effect was negligible. In the inset, the portion of the curve where ln(resistance^{-1}) versus $1/\sqrt{t}$ is linear is shown, where t is the deposition time. A fit to the tunnelling expression is shown as a solid red line. See text for details.*

off or attenuation factor [20, 21]. A fit of this equation to the inverse of the resistance is shown in the inset of Fig. 4. In the 26–150 kΩ region the fit is good indicating that the tunnelling distance between adjacent nanoparticles decreases steadily during this stage of the deposition. To establish a fit, requires determining the proportionality factor A for $d = At^{-1/2}$, which was done by measuring interparticle distance d at specific time t using STM imaging of Ag nanoparticles on HOPG. From such fits to a number of data sets, the value of β obtained is 0.67 $Å^{-1}$. This value compares well with literature values that are typically 0.6–1.0 $Å^{-1}$ [3]. The good comparison indicates that tunnelling is the dominant mechanism of charge transport in the nanoparticle films with comparable interparticle separations.

The addition of molecules to the particle surfaces or interparticle spaces is expected to change the rate of tunnelling and thus the resistance of the nanoparticle film. To effect such change, the nanoparticles were exposed to 2-CEES. A sample of the change in film resistance that resulted during the exposure is shown in Fig. 5. As seen, within 1 min of opening a bottle of 2-CEES positioned 5 cm away, in a fume hood through which air was flowing at a rate greater than 500 ft^3 min^{-1}, the resistance across the film had changed. Furthermore, the resistance decreased from 6 MΩ to 160 kΩ within 8 min. The large change suggests high sensitivity.

To gauge the sensitivity, the change in resistance and the change in the optical properties of some nanoparticle films were monitored simultaneously. Some sample results of the optical and resistance data obtained are shown in Fig. 6. The absorption spectrum has a peak absorbance near 750 nm, corresponding to the surface plasmon resonance (SPR) of the nanoparticles [19]. The position of the SPR is known to be very sensitive to the presence of adsorbates on the nanoparticle surface. For example, picograms of 2-CEES could be detected by monitoring the shift in the SPR of Au nanoparticles [22]. In Fig. 6, no shift in the SPR is observable. By comparison, the resistance changes by more than 1 MΩ. It is clear that under these conditions the change in resistance is much more sensitive to the presence of 2-CEES than is the SPR peak position. Future work will focus on quantifying the detection limit of the resistance measurement. The purpose of the present work is to demonstrate that measurement of the resistance across high density nanoparticle films is promising as a highly sensitive, portable sensor platform.

Following exposure to 2-CEES, the resistance of the nanoparticle films decreased significantly, as seen in Fig. 6, and stayed there. The effect was irreversible. Heating of the films was not possible because the polyethylene melts and swells at relatively low temperatures, which would drastically alter the interparticle spacing and conduction characteristics of the nanoparticle film. Letting the films off-gas by leaving the films to sit for several days had no effect; 2-CEES irreversibly adsorbed to the nanoparticles. In this context, the nanoparticle films function as cumulative sensors. Exposure of such sensors to trace amounts of toxic chemicals, such as 2-CEES, results in a steady build up of the toxic chemical on the surfaces of the nanoparticles. Eventually, the build up causes a change in resistance large enough to be measured. The disadvantage of cumulative sensing is that the sensor is destroyed in the process. The advantage is that cumulative sensors can detect trace quantities of toxic gas well below the detection threshold of concentration-based, one-time sampling techniques.

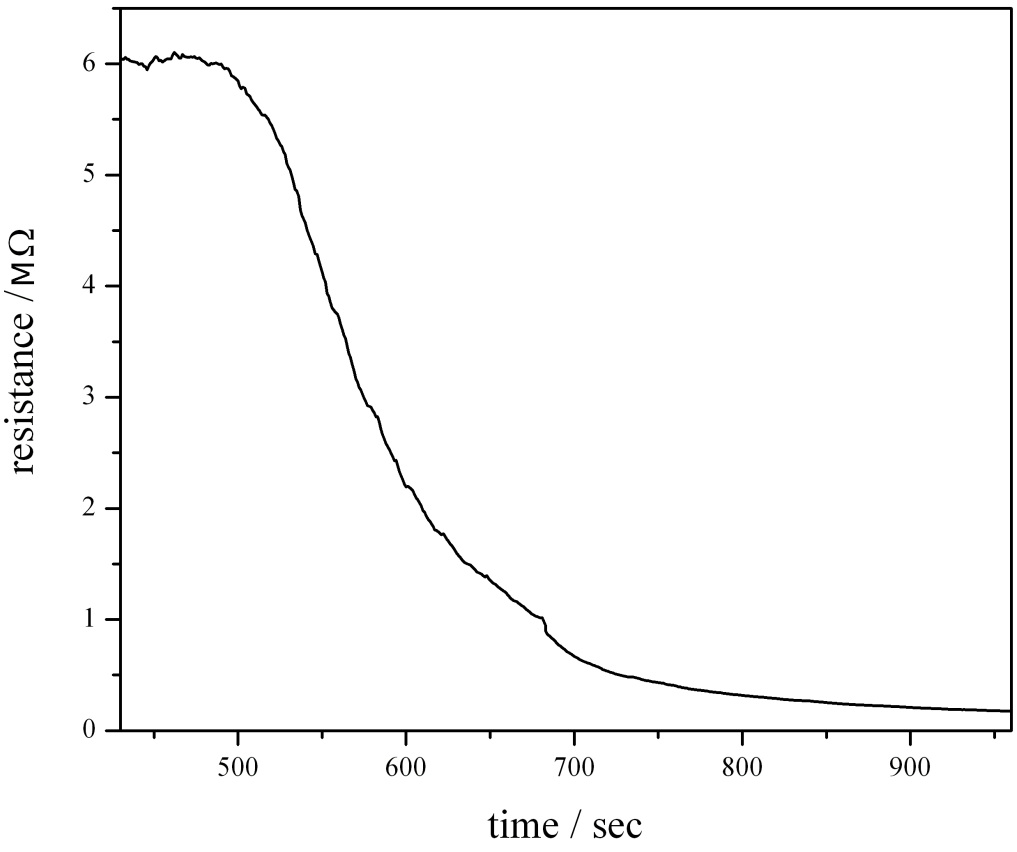

Figure 5: *Plot of the resistance, between two Ag electrodes painted onto a 5 μm thick polyethylene film, versus the time of exposure to 2-CEES. The electrodes were 3 mm apart. The 2-CEES exposure started at 480 s.*

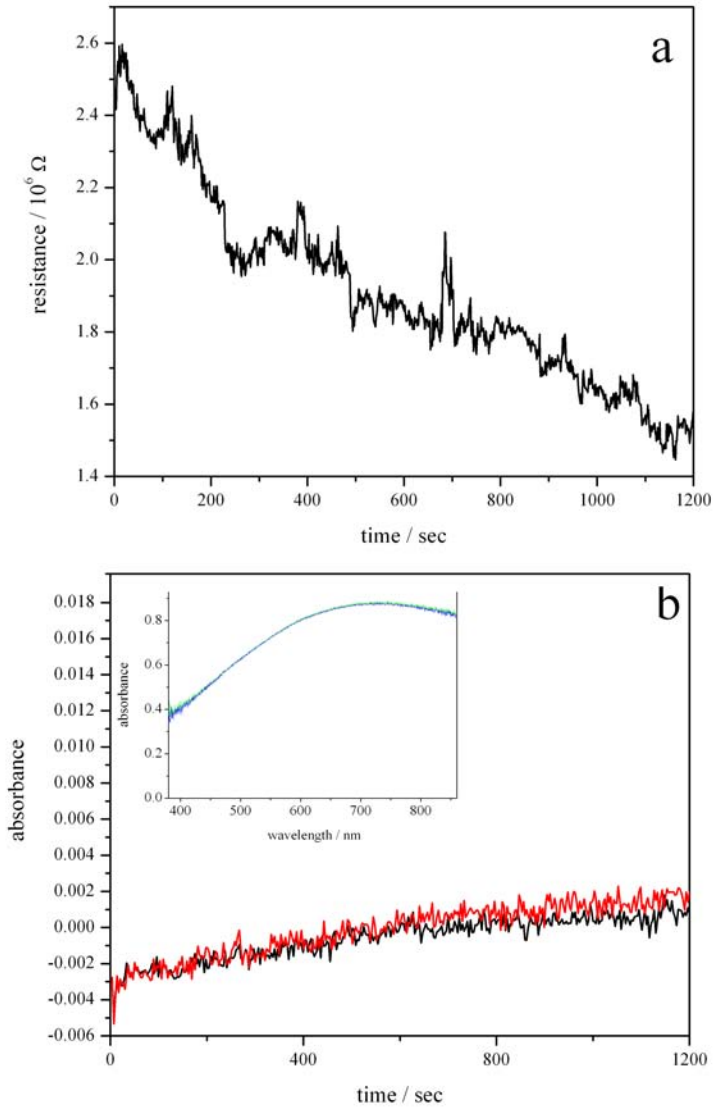

Figure 6: *In* a *the resistance across a Ag nanoparticle film is shown as a function of the exposure time to 2-CEES. The resistance data were acquired simultaneously with the absorbance data shown in* b*. In the inset in* b *the absorbance spectrum is shown before (blue) and after (green) the exposure. The red and black traces in the main figure of* b *show the change in absorbance measured at 700 and 650 nm, respectively, as a function of exposure time* t*.*

Furthermore, the cumulative sensor response changes steadily with time thus providing a continuous readout related to the total amount of toxic chemical that the sensor has encountered over the total period of exposure. In light of these sensing properties and the highly portable nature of the nanoparticle films, measurements of resistance across these films is very promising as a portable sensor platform suitable for use as personal exposure indicators and other related devices.

4 Summary and Conclusions

Gas-phase Ag nanoparticles deposit readily onto glass and polyethylene substrates forming monolayer films. The distance between nanoparticles in these films can be controlled such that sequential tunnelling of electrons between adjacent nanoparticles is the dominant means of current flow through the film. Under these conditions, electrons necessarily tunnel through the interparticle spaces and the resistance across the film is very sensitive to changes in these spaces. Adsorption of gas onto the nanoparticle films, for example, was found to significantly alter the conduction characteristics. Exposure to 2-CEES (a simulant of the chemical warfare agent sulfur mustard), was found to cause more than order-of-magnitude changes in the resistance measured across the nanoparticle films. In this context the nanoparticle films make promising sensor platforms. Portability, low power requirements, and high sensitivity are potential advantages of such sensors. In the case of 2-CEES, adsorption is irreversible, so the nanoparticle films function as cumulative sensors. Because the 2-CEES is continuously adsorbed, the change in resistance across the nanoparticle film is directly related to the total exposure incurred over the entire exposure time. Although the sensors may have multiple uses, in light of their properties they are most appealing as badge-type personal exposure indicators.

References

[1] Kwok, K. and Ellenbogen, J.C. (2002), Moletronics: Future Electronics, *Mat. Today*, 5(2), 28–37.

[2] Das, S., Rose, G., Ziegler, M.M., Picconatto, C.A., and Ellenbogen, J.C. (2005), Architectures and Simulations for Nanoprocessor Systems Integrated on the Molecular Scale. in Cunibert, G; Fagas, G; and Richter, K., *Introducing Molecular Electronics*, Springer-Verlag, Berlin.

[3] Adams, D.M., Brus, L., Chidsey, C.E.D., Creager, S., Creutz, C., Kagan, C.R., Kamat, P.V., Lieberman, M., Lindsay, S., Marcus, R.A., Metzger, R.M., Michel-Beyerle, M.E., Miller, J.R., Newton, M.D., Rolison, D.R., Sankey, O., Schanze, K.S., Yardley, J., and Zhu, X. (2003), Charge Transfer on the Nanoscale: Current Status, *J. Phys. Chem. B*, 107, 6668–6697.

[4] Feldheim, D.L. and Keating, C.D. (1998), Self-assembly of single electron transistors and related devices, *Chem Soc. Rev.*, 27, 1–12.

[5] Schmid, G., (Ed.) (2004), Nanoparticles, From Theory to Application, pp 328-369, Wiley-VCH. Verlag GmbH and Co. KGaA. Weinheim, Germany.

[6] Jortner, J., Bixon, M., Langenbacher, T., and Michel-Beyerle, M.E. (1998), Charge transfer and transport in DNA, *Proc. Natl. Acad. Sci.*, 95, 12759–12765.

[7] Selzer, Y., Salomon, A., and Cahen, D. (2002), The importance of chemical bonding to the contact for tunnelling through alkyl chains, *J. Phys. Chem. B*, 106, 10432–10439.

[8] Taleb, A., Silly, F., Gusev, A.O., Charra, F., and Pileni, M.-P. (2000), Electron transport properties of nanocrystals: isolated and "supra"-crystalline phases, *Adv. Mater.*, 12(9), 633–637.

[9] Kim, S.-H., Medeiros-Ribeiro, G., Ohlberg, D.A.A., Williams, R.S., and Heath, J.R. (1999), Individual and collective electronic properties of Ag nanocrystals, *J. Phys. Chem. B*, 103, 10341–10347.

[10] Markovich, G., Collier, C.P., and Heath, J.R. (1998), Reversible Metal-Insulator Transition in Ordered Metal Nanocrystal Monolayers Observed by Impedance Spectroscopy, *Phys. Rev. Lett.*, 80(17), 3807–3810.

[11] Chi, L.F., Hartig, M., Drechsler, T., Schaak, T., Seidel, C., Fuchs, H., and Schmid, G. (1998), *Appl. Phys. Lett. A*, 66, 187.

[12] Chen, S. (2000), Self-assembling of monolayer-protected gold nanoparticles, *J. Phys. Chem. B*, 104, 663–667.

[13] Andres, R.P., Bein, T., Dorogi, M., Feng, S., Henderson, J.I., Kubiak, C.P., Mahoney, W., Osifchin, R.G., and Reifenberger, R. (1996), Coulomb Staircase at Room Temperature in a Self-Assembled Molecular Nanostructure, *Science*, 272(5266), 1323 – 1325.

[14] Reed, M.A., Zhou, C., Muller, C.J., Burgin, T.P., and Tour, J.M. (1997), Conductance of a Molecular Junction, *Science*, 278, 252.

[15] Chen, J., Reed, M.A., Rawlett, A.M., and Tour, J.M. (1999), Large On-Off Ratios and Negative Differential Resistance in a Molecular Electronic Device, *Science*, 286, 1550.

[16] Pedersen, D.B. and Wang, S. (2007), Iodination of Gas-Phase-Generated Ag Nanoparticles: Behavior of the Two Spin Orbit Components of the AgI Exciton in Ag@AgI Core-Shell Nanoparticles, *J. Phys. Chem. C*, 111, 1261–1267.

[17] Heiz, U. and Schneider, W.-D. (2000), Nanoassembled model catalysts, *J. Phys. D.: Appl. Phys.*, 33, R85–R102.

[18] Pedersen, D.B. and Wang, S. (2009), Remarkably Strong Interparticle Coupling in Two-Dimensional Ensembles of Naked Silver Quantum Dots: The Effect on Optical and Conduction Characteristics, *J. Phys. Chem. C*, 113, 4797–4803.

[19] Pedersen, D.B., Wang, S., Paige, M.F., and Leontowich, A.F.G. (2007), Exploiting Near-Field Coupling between Closely Spaced, Gas-Phase, 10 ± 5 nm Ag Nanoparticles Deposited on NaCl To Observe the Quadrupolar Surface Plasmon Absorption, *J. Phys. Chem. C.*, 111, 5592–5598.

[20] Nunez, M.E., Hall, D.B., and Barton, J.K. (1997), Long-range oxidative damage to DNA: effects of distance and sequence, *Chem. Biol.*, 6, 85–97.

[21] Lewis, F.D., Wu, T., Liu, X., Letsinger, R.L., Greenfield, S.R., Miller, S.E., and Wasielewski, M.R. (2000), Dynamics of photoinduced charge separation and charge recombination in synthetic DNA hairpins with stilbenedicarboamide linkers, *J. Am. Chem. Soc.*, 122, 2889–2902.

[22] Pedersen, D. B. and Duncan, E. J. S. (2005), Surface plasmon resonance spectroscopy of gold nanoparticle-coated substrates, (DRDC Suffield TR 2005-109) Defence R&D Canada–Suffield.

This page intentionally left blank.

DOCUMENT CONTROL DATA

(Security classification of title, body of abstract and indexing annotation must be entered when document is classified)

1. ORIGINATOR (the name and address of the organization preparing the document. Organizations for whom the document was prepared, e.g. Centre sponsoring a contractor's report, or tasking agency, are entered in section 8.)

   Defence R&D Canada – Suffield
   Box 4000, Station Main, Medicine Hat, Alberta,
   Canada T1A 8K6

2. SECURITY CLASSIFICATION (overall security classification of the document including special warning terms if applicable).

   UNCLASSIFIED

3. TITLE (the complete document title as indicated on the title page. Its classification should be indicated by the appropriate abbreviation (S,C,R or U) in parentheses after the title).

   Current flow through two dimensional arrays of metal nanoparticles as a novel sensor platform

4. AUTHORS (last name, first name, middle initial)

   Pedersen, D.B.; Wang, S.

5. DATE OF PUBLICATION (month and year of publication of document)	6a. NO. OF PAGES (total containing information. Include Annexes, Appendices, etc).	6b. NO. OF REFS (total cited in document)
May 2009	24	22

7. DESCRIPTIVE NOTES (the category of the document, e.g. technical report, technical note or memorandum. If appropriate, enter the type of report, e.g. interim, progress, summary, annual or final. Give the inclusive dates when a specific reporting period is covered).

   Technical Memorandum

8. SPONSORING ACTIVITY (the name of the department project office or laboratory sponsoring the research and development. Include address).

   Defence R&D Canada – Suffield
   Box 4000, Station Main, Medicine Hat, Alberta, Canada T1A 8K6

9a. PROJECT NO. (the applicable research and development project number under which the document was written. Specify whether project).	9b. GRANT OR CONTRACT NO. (if appropriate, the applicable number under which the document was written).

10a. ORIGINATOR'S DOCUMENT NUMBER (the official document number by which the document is identified by the originating activity. This number must be unique.)	10b. OTHER DOCUMENT NOs. (Any other numbers which may be assigned this document either by the originator or by the sponsor.)
DRDC Suffield TM 2009-068	

11. DOCUMENT AVAILABILITY (any limitations on further dissemination of the document, other than those imposed by security classification)

    (X) Unlimited distribution
    ( ) Defence departments and defence contractors; further distribution only as approved
    ( ) Defence departments and Canadian defence contractors; further distribution only as approved
    ( ) Government departments and agencies; further distribution only as approved
    ( ) Defence departments; further distribution only as approved
    ( ) Other (please specify):

12. DOCUMENT ANNOUNCEMENT (any limitation to the bibliographic announcement of this document. This will normally correspond to the Document Availability (11). However, where further distribution beyond the audience specified in (11) is possible, a wider announcement audience may be selected).

    Unlimited

13. ABSTRACT (a brief and factual summary of the document. It may also appear elsewhere in the body of the document itself. It is highly desirable that the abstract of classified documents be unclassified. Each paragraph of the abstract shall begin with an indication of the security classification of the information in the paragraph (unless the document itself is unclassified) represented as (S), (C), (R), or (U). It is not necessary to include here abstracts in both official languages unless the text is bilingual).

Exposure of nanoparticles of Ag to 2-CEES (2-chloroethyl ethylsulfide, a simulant of the sulfur mustard warfare agent) was found to cause a significant change in the film conduction characteristics that could be used as a sensitive method of detection. Ag nanoparticles deposited onto highly-ordered pyrolitic graphite, glass, and polyethylene substrates were found to form such films. Uptake of 2-CEES was irreversible and cumulative. The sensitivity and cumulative nature make the nanoparticle films most appealing as personal exposure indicators.

14. KEYWORDS, DESCRIPTORS or IDENTIFIERS (technically meaningful terms or short phrases that characterize a document and could be helpful in cataloguing the document. They should be selected so that no security classification is required. Identifiers, such as equipment model designation, trade name, military project code name, geographic location may also be included. If possible keywords should be selected from a published thesaurus. e.g. Thesaurus of Engineering and Scientific Terms (TEST) and that thesaurus-identified. If it not possible to select indexing terms which are Unclassified, the classification of each should be indicated as with the title).

sensors
nanoparticles
electronics

Defence R&D Canada

Canada's Leader in Defence
and National Security
Science and Technology

R & D pour la défense Canada

Chef de file au Canada en matière
de science et de technologie pour
la défense et la sécurité nationale

www.drdc-rddc.gc.ca